ARTICLE

The antimicrobial action of silver nanoparticles on *Escherichia coli* as revealed by atomic force microscopy

Eloise I. Prieto* and Analiza A. Kiat

National Institute of Molecular Biology and Biotechnology, National Science Complex,
College of Science, University of the Philippines Diliman, Quezon City, 1101 Philippines

The antimicrobial nature of silver nanoparticles (AgNPs) has been exploited commercially due to its broad spectrum activity. Although AgNPs are currently incorporated into numerous medical and consumer products, their action against microbes is not yet fully elucidated. This study investigated the antibacterial activity and mechanism of AgNP on Gram-negative *E. coli* through analysis of the growth characteristics, permeability, and morphology of AgNP-treated cells. The minimum inhibitory concentration and half-inhibitory concentration of the AgNPs were found to be 55.56 μg ml^{-1} and 21.23 μg ml^{-1}, respectively. Treatment of *E. coli* with AgNP altered membrane potential and compromised membrane integrity. Time course analysis of treated cells through atomic force microscopy (AFM) revealed nanometer-scale details of *E. coli* response to AgNP. Images showed that disruption of the outer membrane structure is an early event that precedes damage and disintegration of both *E. coli* membranes and leakage of its cytoplasmic content. Morphological analysis revealed that hallmarks of cell damage and AgNP toxicity include increase in cell surface roughness and decrease in both cell height and length. The study was able to provide a clearer picture on the membrane-based toxicity mechanism of AgNP by revealing details of AgNP-mediated membrane damage on *E. coli* cells.

KEYWORDS

silver nanoparticles, atomic force microscopy, antimicrobial activity

INTRODUCTION

Silver nanoparticles (AgNPs) are the most commercialized nanomaterial due to their well-established broad spectrum antimicrobial properties and their lower tendency to induce microbial resistance (Kim, Kuk, et al. 2007). Unlike their macro and micro counterparts, nanoparticles demonstrate unique physical and chemical properties due to their high surface area and nanometer size, making them suitable antimicrobial agents. Products that incorporate AgNPs include wound dressings, medical devices, and textile fabrics (Thomas, et al. 2007; Rai, et al. 2009; Mohite and Patil 2016). The antimicrobial activity of AgNPs has been attributed to the following: (i) release of silver ions which interfere with membrane potential, protein function, and DNA replication (Morones, et al. 2005; Xiu, et al. 2012; Franci, et al. 2015) , (ii) particle-specific effects or direct physical contact between AgNPs and microorganisms that damages the membrane (Sondi and Salopek-Sondi 2004; Bondarenko, et al. 2013), and (iii) generation of reactive oxygen species (ROS) compromising membrane integrity (Kim, Lee, et al. 2007). It is acknowledged that the physical characteristics of AgNPs such as size and specific area affect their antimicrobial

*Corresponding author
Email Address: prieto.eloise@mbb.upd.edu.ph
Date received: September 16, 2017
Date revised: November 28, 2017
Date accepted: December 14, 2017

activity (Pal, et al. 2007; Kvítek, et al. 2008; Prabhu and Poulose 2012; Tejamaya, et al. 2012). Smaller-sized AgNPs have been found to have better antimicrobial properties compared to larger-sized AgNPs due to the higher intracellular bioavailability of silver caused by greater cell-particle contact and increased release of silver ions (Kim, Kuk, et al. 2007; Lu, et al. 2013; Ivask, et al. 2014; Raza, et al. 2016; Molleman and Hiemstra 2017).

Membrane damage is widely accepted as one of the mechanisms by which AgNPs exert their toxic effects on microorganisms. Morphological changes on microbes treated with AgNP have been observed such as formation of pores and release of cytoplasmic content (Sondi and Salopek-Sondi 2004; Pal, et al. 2007; Li, et al. 2010; Prabhu and Poulose 2012; Ramalingam, et al. 2016). However, the details behind AgNP-mediated membrane damage that lead to cell death is still unclear. A better understanding of the antimicrobial mechanism of AgNP is critical in advancing the development of antimicrobial materials with AgNPs as well as clarify their potential environmental impact. This study therefore aimed to gain insight on the AgNP mechanism of action.

Atomic force microscopy (AFM) is a powerful imaging technique capable of providing nanometer-scale resolution images of biological samples even under physiological conditions. AFM has been successfully used in studying the mechanism of action of antimicrobials on cells (da Silva and Teschke 2003; Li, et al. 2007; Eaton, et al. 2008; Alves, et al. 2010; Wang, et al. 2016). This study utilized AFM to examine the mechanism of antimicrobial action of AgNPs against the Gram-negative bacterium *E. coli*. Time course visualization of AgNP-treated cells was done to dissect AgNP-mediated morphological and structural changes. Through AFM analysis, this study was able to obtain significant insights on the antimicrobial activity of AgNP. Images obtained demonstrated that perturbation of the *E. coli* membrane is an important early step in AgNP antimicrobial activity, followed by destruction of the cell membrane leading to cytoplasm leakage and eventual cell death. Moreover, morphological indicators of AgNP toxicity were identified, specifically, cell surface roughness, cell height, and cell length.

MATERIALS AND METHODS

Materials

Spherical polyvinylpyrrolidone (PVP)-coated 5 nm silver nanoparticles (AgNP) were purchased from Nanocomposix Incorporated (United States) as 1 mg ml^{-1} stock solutions. The nanoparticles were stored at 4°C away from light until use. Luria–Bertani (LB) medium (Scharlau Chemie SA) was used in growing and maintaining the bacterial culture. *Escherichia coli* O157:H7 strain SS52 was obtained from the Philippine National Collection of Microorganisms, Biotech, University of the Philippines Los Baños.

Characterization of AgNP stability

The stability of the PVP-coated 5 nm AgNP was evaluated in distilled water and LB broth through absorption spectroscopy. The absorbance spectra (300 nm to 800 nm) of 100 µg ml^{-1} AgNP solutions were measured at 0 and 24 hours of incubation at 37°C. The absorbance was recorded at 2 nm increments.

Determination of the AgNP antimicrobial property

The minimum inhibitory concentration (MIC) was determined using the broth microdilution method. A series of three-fold serial dilutions of AgNP in LB broth were made starting from 500 µg ml^{-1} to 0.008 µg ml^{-1}. Bacteria were inoculated at 5 x 10^5 cells ml^{-1}. The effect of AgNPs on bacterial growth was measured spectrophotometrically at 600 nm for 12 hours at 2 hour intervals, and after 24 hours. A blank control (culture medium with AgNP) was included in every experiment. Growth curves were then constructed. The IC_{50} was calculated with the Excel macro REGTOX (Vindimian 2003).

Detection of Membrane Damage

To determine the ability of AgNPs to confer membrane damage, cultured *E. coli* cells treated with increasing concentrations of AgNP were stained with BacLight Bacterial Viability Kit (Molecular Probes) according to manufacturer's instructions. Fluorescence ratio of Syto 9 to PI was measured to quantify membrane damage. Representative samples were also imaged using Olympus BX51 with FITC and TXRED filters.

AFM imaging

Cultured *E. coli* cells were treated with AgNP at IC_{50} concentration and collected at different time points (0, 10, 120, 360 minutes). Cell suspensions were placed onto a glass cover slip and dried using nitrogen gas. The sample was then washed with deionized distilled water and dried. Untreated bacteria were prepared in a similar manner and used as control. Non-contact mode AFM was performed in air using XE-Bio AFM (Park Systems). Silicon/aluminum coated cantilevers (PPP-NCHR 10 M; Park Systems) with a typical spring constant of 42 N m^{-1} were used to image both AgNP-treated and untreated *E. coli*. Images were captured in a 512 x 512 pixel format, plane-fitted, and flattened by the software supplied with the imaging module (XEI, Park Systems). Cell surface roughness, cell height, and cell length were measured from the images obtained using the XEI software (Park Systems). The root-mean-square (RMS) average of the surface roughness value obtained was defined as the standard deviation of all the height values within the given area while the height of the cell was defined as the difference between the top and bottom heights of the cell.

Statistical analysis

For membrane damage and AFM analysis, reported values refer to averages of three independent experiments using at least three replicates for each group. Analysis of variance (ANOVA) method followed by Dunnett's post-hoc test was done to determine statistical significance.

RESULTS AND DISCUSSION

Stability of silver nanoparticles

This study utilized 5 nm AgNP stabilized with PVP because these have been proven to have a better antimicrobial activity than their larger-sized counterparts due to their larger surface area and stability (Lu, et al. 2013; Raza, et al. 2016). Because the efficacy of nanoparticles as antimicrobial agents depends on their physical properties as well as the environment they are in (Pal, et al. 2007; Kvítek, et al. 2008; Prabhu and Poulose 2012; Tejamaya, et al. 2012), stability of AgNPs in culture medium (LB broth) was initially determined through absorption spectroscopy. AgNPs in water served as a control. Silver nanoparticles in water and LB broth displayed prominent peaks at approximately 400 nm, characteristic of its surface plasmon resonance (SPR) indicating the presence of the nanoparticles (Fig. 1).

A slight decrease and red-shift on the absorbance profile of AgNPs in LB was noted. This may be due to media components such as proteins and peptides that readily adsorb onto the AgNPs. The SPR peaks of AgNPs in both water and LB were still present after 24 hours of incubation indicating that the AgNPs are stable under experimental conditions.

Antimicrobial action of silver nanoparticles on E. coli

Growth kinetics of *E. coli* was monitored in the presence of AgNPs to characterize their antimicrobial activity against Gram-

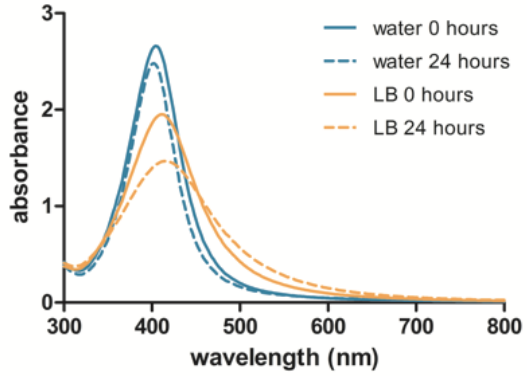

Figure 1: UV-Vis absorption spectra of 100 μg ml^{-1} 5 nm AgNP in distilled water (blue) and LB broth (orange) at 0 (solid lines) and 24 (dashed lines) hours of incubation.

negative bacteria. The antimicrobial activity of AgNPs was dose dependent and resulted in growth inhibition of cultured cells (Fig. 2). The minimum inhibitory concentration (MIC) was found to be 55.56 μg ml^{-1}. A half-inhibitory concentration (IC_{50}) of 21.23 μg ml^{-1} was obtained.

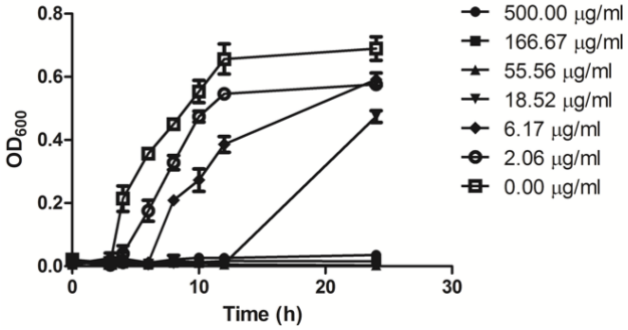

Figure 2: Growth profile of *E. coli* treated with AgNP. Untreated cells served as negative control.

The ability of AgNPs to confer membrane damage was assessed with BacLight Bacterial Viability Kit (Molecular Probes). The assay makes use of fluorescent dyes propidium iodide (PI) and Syto 9. Membrane permeability to these dyes depends on cell membrane potential providing a method for distinguishing viable from dead cells. The red fluorescent dye PI only permeates cells with damaged membranes because of their altered membrane potential. In contrast, the green fluorescent dye Syto 9 stains both live and dead bacteria. Live bacteria will therefore fluoresce green while cells with damaged membranes will exhibit red fluorescence. Although both untreated and AgNP-treated cells stained green (Fig. 3a and c, respectively), only *E. coli* cells treated with AgNP stained red (Fig 3d), demonstrating the ability of AgNPs to damage bacterial membrane. Membrane damage was quantified through the ratio of emission at 530 nm for Syto 9 and 630 nm for PI. A concentration-dependent decrease of Syto 9 to PI emission ratios were obtained for AgNP-treated bacteria (Fig. 3e). This confirms bacterial membrane damage from AgNP treatment.

Structural effect of AgNP on E. coli over time

It has been consistently shown that membrane damage caused by AgNP contributes to the antimicrobial action of these nanomaterials (Sondi and Salopek-Sondi 2004; Kim, Kuk, et al. 2007; Pal, et al. 2007; Li, et al. 2010; Prabhu and Poulose 2012). However, structural changes on the cell membrane after AgNP treatment leading up to damage and eventual cell death remain vague. To elucidate the mechanism of AgNP-mediated cell

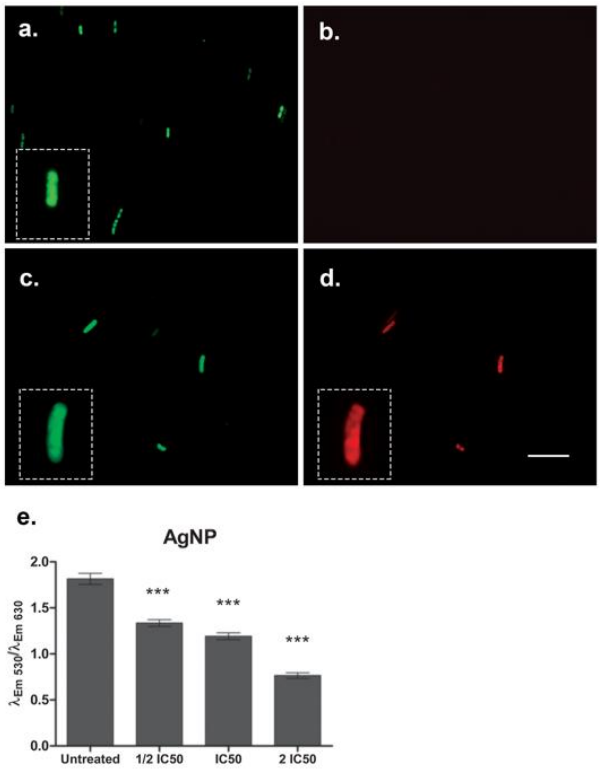

Figure 3: Effect of AgNP on cell membrane integrity. Fluorescence microscopy images with magnified cells (inset) of (a)-(b) untreated and (c)-(d) AgNP-treated *E. coli* cells after using BacLight Bacterial Viability Kit (Molecular Probes). Live cells with intact membrane are green while cells with compromised membrane stain red. Scale bar = 80 μm. (e) Quantified effect of AgNP on *E. coli* cells. Statistical significance was assayed by one-way ANOVA, followed by Dunnett's test. $^{***}p<0.001$.

damage on *E. coli*, the structural and morphological changes of AgNP-treated cells were investigated at different time points through AFM.

Images of untreated *E. coli* showed the characteristic rod shape of the bacterium with an average cell length of 3.57 ± 0.17 μm (n=40) (Fig. 4). Line section profile of the cell as well as its magnified images depict an intact and relatively smooth cell surface. This indicates that the *E. coli* cell membrane is

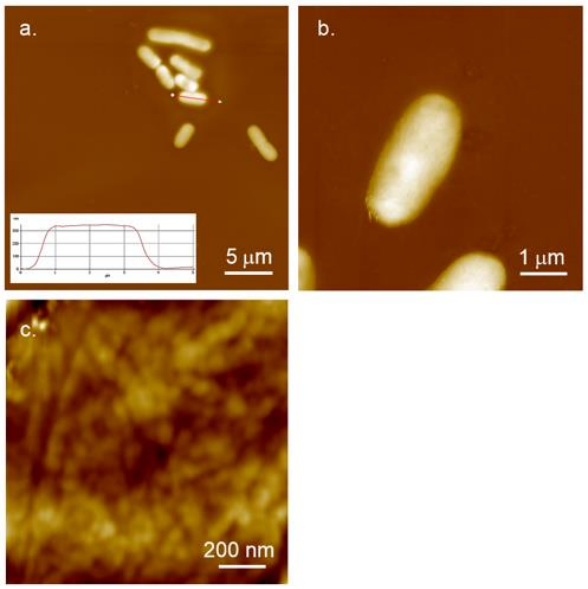

Figure 4: AFM images of untreated *E. coli* cells. (a) Topographical image with line profile analysis showing an intact and smooth cell surface, (b)-(c) magnified images of an *E. coli* cell showing its surface morphology.

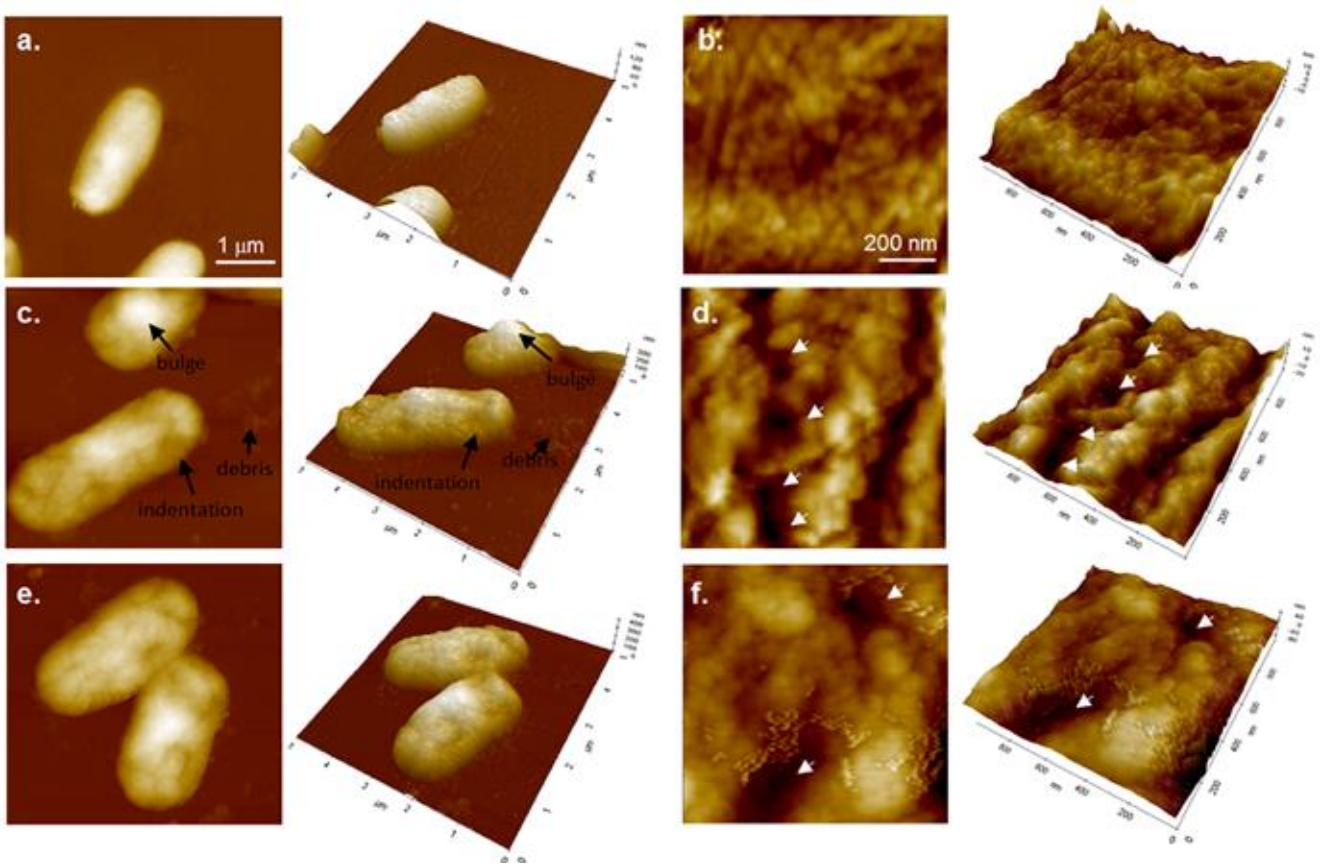

Figure 5: AFM images of *E. coli* 10 minutes after AgNP treatment showing gross (a), (c), and (e) and detailed (b), (d), and (f) cell surface properties of (a)-(b) untreated and (c)-(f) AgNP-treated cells. Indentations and bulges (black arrows) as well as nanopores (white arrowheads) indicate cell damage. Left panels: height images, right panels: 3D reconstruction based on height data.

undamaged and the processing method for AFM imaging does not substantially affect cell structure and morphology. On the other hand, significant changes on the cell morphology of AgNP-treated *E. coli* cells were noted. Bulges, indentations, and some nanopores appeared on the cell surface 10 minutes after AgNP treatment (Fig. 5). Some micelle-like structures were also found on the edge of some cells suggesting damage to the *E. coli* outer membrane. Line section analysis revealed an uneven cell surface compared to untreated cells (Fig. 6). The uneven cell surface of the *E. coli* persisted 120 minutes after incubation with AgNPs (Fig. 7). Cell debris were also noted as collapsed cell structures in the images indicating the presence of dead cells even after only 120 minutes of incubation with AgNPs.

These local deformations may be due to lipid restructuring as nanoparticles interact with cell membrane (Wang, et al. 2008; Chen and Bothun 2011). Nanoparticle-treated microbes have been demonstrated to have a reduced lipid density and variations in the plasma membrane content (Leroueil, et al. 2007) which can affect cell surface morphology. Additionally, chemical analysis have demonstrated that AgNP can alter lipopolysaccharide and phosphatidylethanolamine structure, the major phospholipid components of the *E. coli* outer membrane

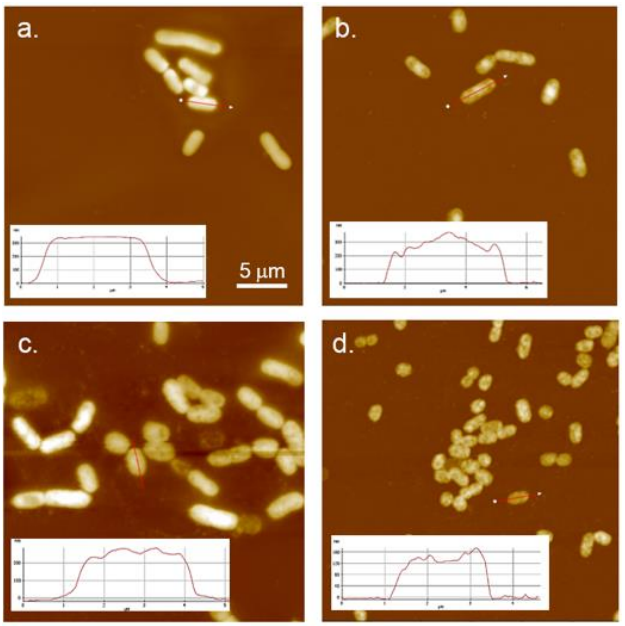

Figure 6: AFM images of (a) untreated *E. coli* cells and cells treated with AgNP for (b) 10, (c) 120, and (d) 360 minutes with line section profiles (red lines) showing a rougher cell surface for treated cells.

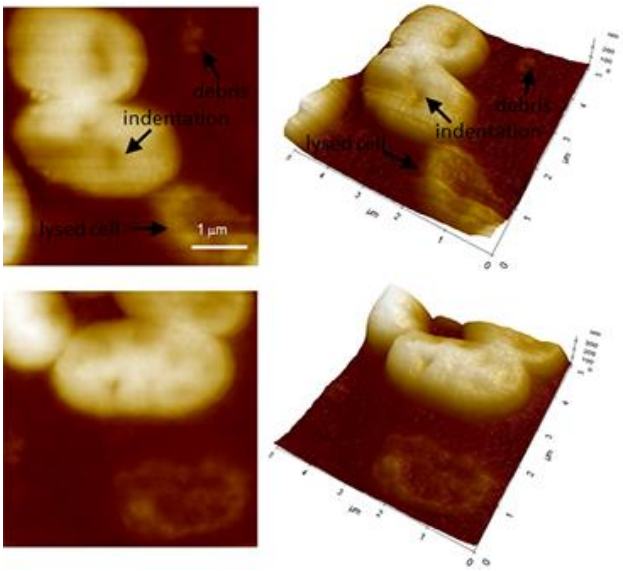

Figure 7: AFM images of morphological changes occurring on *E. coli* cell surface 120 minutes after AgNP treatment. Left panel: topographical images, right panel: 3D reconstructions based on height data.

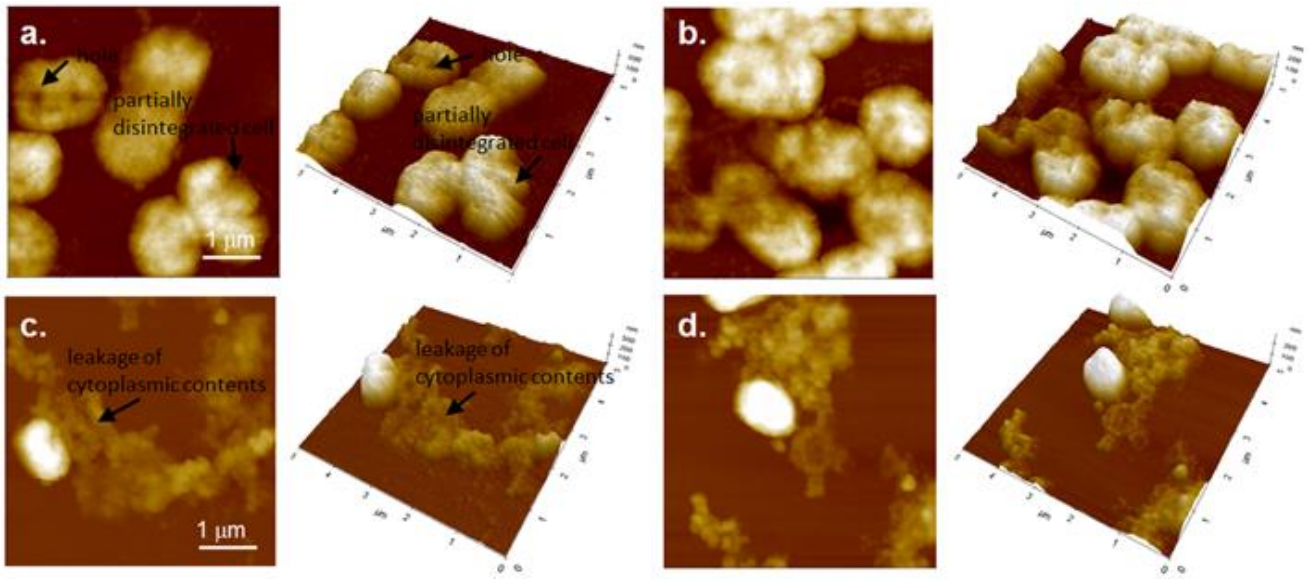

Figure 8: AFM images of *E. coli* 360 minutes after AgNP treatment showing (a)-(b) holes and indentation on the cell surface, partially disintegrated cells with damaged membrane structures, and (c)-(d) leakage of cytoplasmic contents. Left panel: topographical images, right panel: 3D reconstructions based on height data.

(Ansari, et al. 2014). Damage to outer membrane proteins may also contribute to perturbations in membrane structure of AgNP-treated cells. The interaction of silver with thiol groups of membrane proteins has been shown to alter the structure and function of these proteins (Feng, et al. 2000; Jung, et al. 2008; Rai, et al. 2009). The ability of AgNP to destabilize *E. coli* outer membrane and disrupt outer membrane components is further supported by a study that utilized proteomic analysis of AgNP-treated cells. It showed induced expression of envelope proteins integral in safeguarding the cell against entry of foreign substances (Vaara 1992; Lok, et al. 2006).

The transient voids and pores formed in the *E. coli* outer membrane after AgNP treatment lead to changes in membrane permeability and membrane leakage (Moghadam, et al. 2012; Li and Malmstadt 2013). This was shown by the increase in PI staining of AgNP-treated *E. coli* cells (Fig. 3). This enhanced membrane permeability lead to an influx of Ag ions from AgNP further compromising cell integrity and facilitating internalization of AgNPs (Sondi and Salopek-Sondi 2004; Morones, et al. 2005; McQuillan, et al. 2012). Passive translocation of nanoparticles has been demonstrated to occur due to membrane invaginations and pores resulting in lipid extraction from the membrane (Brayner, et al. 2006; Peetla and Labhasetwar 2008; Le Bihan, et al. 2009; Chen and Bothun 2011) seen as micelle-like structure coming off the *E. coli* cell (Fig. 5).

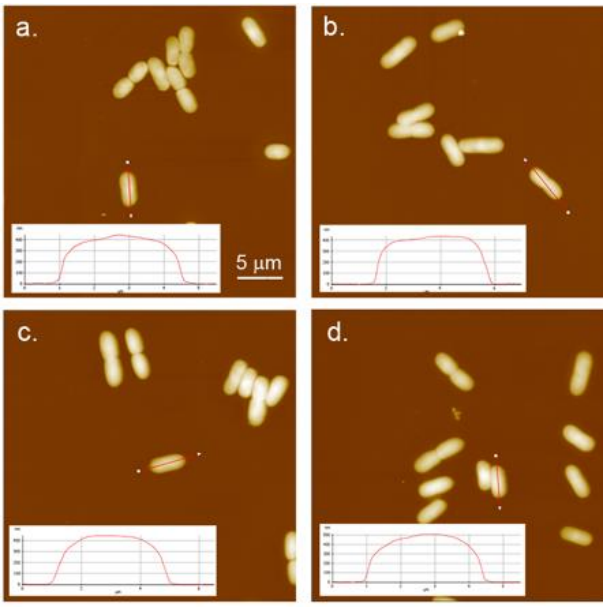

Figure 9: AFM images of untreated *E. coli* cells at different time points: (a) 0, (b) 10, (c) 120, and (d) 360 minutes.

These events were then followed by extensive changes in cell morphology 360 minutes after incubation of *E. coli* with AgNPs (Fig. 8). Most cells have uneven cell surface. Additionally, AgNP-treated cells appear to be disintegrating with copious amount of micelle-like structures coming off of the cells and found around the cells, suggesting further membrane damage. Extensive leakage of cytoplasmic contents were also observed indicating considerable permeabilization and disruption of the *E. coli* peptidoglycan layer and inner membrane. Untreated *E. coli* cells analyzed through AFM at different time points maintained their smooth surface morphology (Figs. 4 and 9). Membrane perturbations were also absent indicating the cells remained intact throughout the analysis and that the visualized structural changes were due to AgNP treatment (Fig. 9).

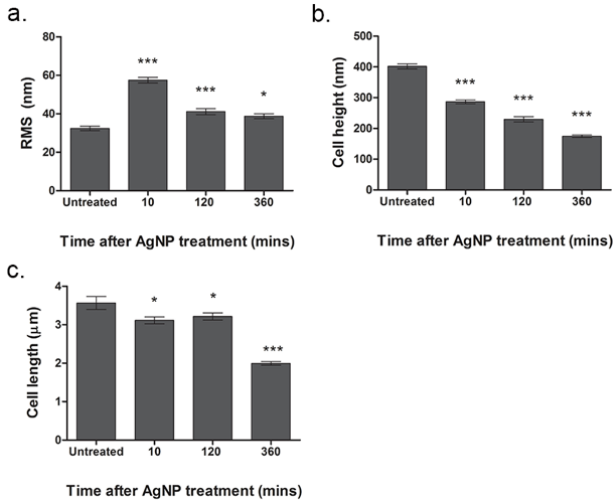

Figure 10: Effect of AgNP treatment on *E. coli* cell morphology. *E. coli* cells treated with AgNPs were imaged and measured using AFM at different time points for (a) surface roughness, (b) cell height, and (c) cell length. Statistical significance was assayed by one-way ANOVA, followed by a Dunnett's test. $^{*}p<0.05$, $^{***}p<0.001$.

Measurement and quantification of alterations in ultrastructural morphology of the cell membrane corroborated the morphological observations made on *E. coli* after AgNP treatment. Untreated *E. coli* cells had significantly lower surface roughness value than AgNP-treated cells (Fig. 10a) confirming the membrane alterations noted in the AgNP-treated cells (Fig. 6) and suggesting membrane damage on the treated cells. A time-dependent decrease in *E. coli* cell height (Fig. 10b) and a significant decrease in cell length (Fig. 10c) were noted after AgNP treatment indicating loss of cell and membrane structure integrity possibly through removal of lipids from the outer membrane. Values obtained from the untreated cells remained constant over time confirming that the variations observed were mediated by AgNP (Fig. 11).

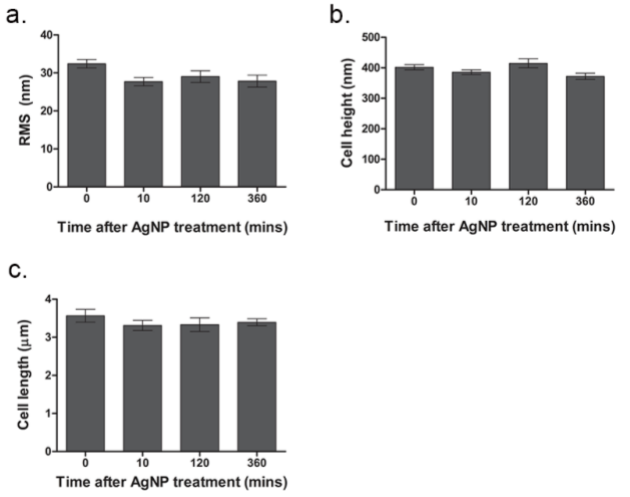

Figure 11: Cell morphology properties of untreated *E. coli* cells at different time points. Untreated *E. coli* cells were imaged and measured for (a) surface roughness, (b) cell height, and (c) cell length using AFM at 0, 10, 120, and 360 minutes post treatment. Statistical significance was assayed by one-way ANOVA, followed by a Dunnett's test.

CONCLUSION

This study showed that 5 nm AgNP-PVP is stable in bacterial media and can inhibit *E. coli* growth by compromising membrane integrity of the microorganism. Furthermore, this study has visually demonstrated through AFM imaging the mechanism of AgNP antimicrobial activity in *E. coli*, a representative Gram-negative bacteria. Early events occurring in the outer membrane of *E. coli* indicate that damage to the outer membrane is a critical step in AgNP-mediated antimicrobial activity. This study was also able to demonstrate that cell height, cell length and cell surface roughness are good indicators for assessing antimicrobial activities of materials such as AgNPs.

ACKNOWLEDGMENTS

This work was supported by the Office of the Vice-Chancellor for Research and Development of the University of the Philippines-Diliman (Grant Project No. 141405 PhDIA). The authors would also like to thank Mr. Carlo David Cristobal for assisting in the AFM imaging of the samples.

The authors have no conflict of interest to declare.

CONTRIBUTION OF INDIVIDUAL AUTHORS

EIPrieto conceptualized the study, performed AFM imaging and analyses, analyzed and consolidated the data, and wrote the manuscript. AAKiat performed AgNP stability experiments, antimicrobial assays, and preliminary analysis, and helped in writing the manuscript draft.

REFERENCES

Alves CS, Melo MN, Franquelim HG, Ferre R, Planas M, Feliu L, Bardaji E, Kowalczyk W, Andreu D, Santos NC, et al. *Escherichia coli* cell surface perturbation and disruption induced by antimicrobial peptides BP100 and pepR. J Biol Chem 2010; 285:27536-27544.

Ansari MA, Khan HM, Khan AA, Ahmad MK, Mahdi AA, Pal R, Cameotra SS. Interaction of silver nanoparticles with *Escherichia coli* and their cell envelope biomolecules. J Basic Microbiol 2014; 54:905-915.

Bondarenko O, Ivask A, Kakinen A, Kurvet I, Kahru A. Particle-cell contact enhances antibacterial activity of silver nanoparticles. PLoS One 2013; 8:e64060.

Brayner R, Ferrari-Iliou R, Brivois N, Djediat S, Benedetti MF, Fiévet F. Toxicological impact studies based on *Escherichia coli* bacteria in ultrafine ZnO nanoparticles colloidal medium. Nano Lett 2006; 6:866-870.

Chen Y, Bothun GD. Cationic Gel-phase liposomes with "decorated" anionic SPIO nanoparticles: Morphology, colloidal, and bilayer properties. Langmuir 2011; 27:8645-8652.

da Silva A, Jr., Teschke O. Effects of the antimicrobial peptide PGLa on live *Escherichia coli*. Biochim Biophys Acta 2003; 1643:95-103.

Eaton P, Fernandes JC, Pereira E, Pintado ME, Xavier Malcata F. Atomic force microscopy study of the antibacterial effects of chitosans on *Escherichia coli* and *Staphylococcus aureus*. Ultramicroscopy 2008; 108:1128-1134.

Feng Q, Wu J, Chen G, Cui F, Kim T, Kim J. A mechanistic study of the antibacterial effect of silver ions on *Escherichia coli* and *Staphylococcus aureus*. J Biomed Mate Res 2000; 52:662-668.

Franci G, Falanga A, Galdiero S, Palomba L, Rai M, Morelli G, Galdiero M. Silver nanoparticles as potential antibacterial agents. Molecules 2015; 20:8856-8874.

Ivask A, Kurvet I, Kasemets K, Blinova I, Aruoja V, Suppi S, Vija H, Käkinen A, Titma T, Heinlaan M. Size-dependent toxicity of silver nanoparticles to bacteria, yeast, algae, crustaceans and mammalian cells in vitro. PLoS One 2014; 9:e102108.

Jung WK, Koo HC, Kim KW, Shin S, Kim SH, Park YH. Antibacterial activity and mechanism of action of the silver ion in *Staphylococcus aureus* and *Escherichia coli*. Appl Environ Microbiol 2008; 74:2171-2178.

Kim JS, Kuk E, Yu KN, Kim JH, Park SJ, Lee HJ, Kim SH, Park YK, Park YH, Hwang CY, et al. Antimicrobial effects of silver nanoparticles. Nanomedicine 2007; 3:95-101.

Kim TG, Lee DS, Park TG. Controlled protein release from electrospun biodegradable fiber mesh composed of poly (ε-caprolactone) and poly (ethylene oxide). Int J of Pharm 2007; 338:276-283.

Kvítek L, Panáček A, Soukupová J, Kolář M, Večeřová R, Prucek R, Holecová M, Zbořil R. Effect of surfactants and polymers on stability and antibacterial activity of silver nanoparticles (NPs). J Phy Chem C 2008; 112:5825-5834.

Le Bihan O, Bonnafous P, Marak L, Bickel T, Trépout S, Mornet S, De Haas F, Talbot H, Taveau J-C, Lambert O. Cryo-electron tomography of nanoparticle transmigration into liposome. J Struct Bio 2009; 168:419-425.

Leroueil PR, Hong S, Mecke A, Baker Jr JR, Orr BG, Banaszak Holl MM. Nanoparticle interaction with biological membranes: does nanotechnology present a Janus face? Acc Chem Res 2007; 40:335-342.

Li A, Lee PY, Ho B, Ding JL, Lim CT. Atomic force microscopy study of the antimicrobial action of Sushi peptides on Gram negative bacteria. Biochim Biophys Acta 2007; 1768:411-418.

Li S, Malmstadt N. Deformation and poration of lipid bilayer membranes by cationic nanoparticles. Soft Matter 2013; 9:4969-4976.

Li WR, Xie XB, Shi QS, Zeng HY, Ou-Yang YS, Chen YB. Antibacterial activity and mechanism of silver nanoparticles on *Escherichia coli*. Appl Microbiol Biotechnol 2010; 85:1115-1122.

Lok C-N, Ho C-M, Chen R, He Q-Y, Yu W-Y, Sun H, Tam PK-H, Chiu J-F, Che C-M. Proteomic analysis of the mode of antibacterial action of silver nanoparticles. J Proteome Res 2006; 5:916-924.

Lu Z, Rong K, Li J, Yang H, Chen R. Size-dependent antibacterial activities of silver nanoparticles against oral anaerobic pathogenic bacteria. J Mater Sci Mater Med 2013; 24:1465-1471.

McQuillan JS, Groenaga Infante H, Stokes E, Shaw AM. Silver nanoparticle enhanced silver ion stress response in *Escherichia coli* K12. Nanotoxicology 2012; 6:857-866.

Moghadam BY, Hou W-C, Corredor C, Westerhoff P, Posner JD. Role of nanoparticle surface functionality in the disruption of model cell membranes. Langmuir 2012; 28:16318-16326.

Mohite BV, Patil SV. In situ development of nanosilver-impregnated bacterial cellulose for sustainable released antimicrobial wound dressing. J Appl Biomater Funct Mater 2016; 14:e53-58.

Molleman B, Hiemstra T. Time, pH, and size dependency of silver nanoparticle dissolution: the road to equilibrium. Environ Sci: Nano 2017.

Morones JR, Elechiguerra JL, Camacho A, Holt K, Kouri JB, Ramirez JT, Yacaman MJ. The bactericidal effect of silver nanoparticles. Nanotechnology 2005; 16:2346-2353.

Pal S, Tak YK, Song JM. Does the antibacterial activity of silver nanoparticles depend on the shape of the nanoparticle? A study of the Gram-negative bacterium *Escherichia coli*. Appl Environ Microbiol 2007; 73:1712-1720.

Peetla C, Labhasetwar V. Biophysical characterization of nanoparticle− endothelial model cell membrane interactions. Mol Pharm 2008; 5:418-429.

Prabhu S, Poulose EK. (Prabhu2012 co-authors). Silver nanoparticles: mechanism of antimicrobial action, synthesis, medical applications, and toxicity effects. Int Nano Lett 2012; 2:32.

Rai M, Yadav A, Gade A. Silver nanoparticles as a new generation of antimicrobials. Biotechnol Adv 2009; 27:76-83.

Ramalingam B, Parandhaman T, Das SK. Antibacterial effects of biosynthesized silver nanoparticles on surface ultrastructure and nanomechanical properties of Gram-negative bacteria viz. *Escherichia coli* and *Pseudomonas aeruginosa*. ACS Appl Mater Interfaces 2016; 8:4963-4976.

Raza M, Kanwal Z, Rauf A, Sabri A, Riaz S, Naseem S. Size- and shape-dependent antibacterial studies of silver nanoparticles synthesized by wet chemical routes. Nanomaterials 2016; 6:74.

Sondi I, Salopek-Sondi B. Silver nanoparticles as antimicrobial agent: a case study on *E. coli* as a model for Gram-negative bacteria. J Colloid Interface Sci 2004; 275:177-182.

Tejamaya M, Romer I, Merrifield RC, Lead JR. Stability of citrate, PVP, and PEG coated silver nanoparticles in ecotoxicology media. Environ Sci Technol 2012; 46:7011-7017.

Thomas V, Yallapu MM, Sreedhar B, Bajpai SK. A versatile strategy to fabricate hydrogel-silver nanocomposites and investigation of their antimicrobial activity. J Colloid Interface Sci 2007; 315:389-395.

Vaara M. Agents that increase the permeability of the outer membrane. Microbiol Rev 1992; 56:395-411.

Vindimian E. REGTOX: macro Excel™ for dose-response modelling. 2003. In: France.

Wang B, Zhang L, Bae SC, Granick S. Nanoparticle-induced surface reconstruction of phospholipid membranes. PNAS 2008; 105:18171-18175.

Wang C, Ehrhardt CJ, Yadavalli VK. Nanoscale imaging and hydrophobicity mapping of the antimicrobial effect of copper on bacterial surfaces. Micron 2016; 88:16-23.

Xiu ZM, Zhang QB, Puppala HL, Colvin VL, Alvarez PJ. Negligible particle-specific antibacterial activity of silver nanoparticles. Nano Lett 2012; 12:4271-4275.